

Na-doped β -tricalcium phosphate: physico-chemical and in vitro biological properties

Laëtitia Obadia · Marion Julien · Sophie Quillard ·
Thierry Rouillon · Paul Pilet · Jérôme Guicheux ·
Bruno Bujoli · Jean-Michel Bouler

Received: 7 October 2010 / Accepted: 11 December 2010 / Published online: 8 January 2011
© Springer Science+Business Media, LLC 2010

Abstract Synthetic calcium phosphate ceramics as β -tricalcium phosphate ($\text{Ca}_3(\text{PO}_4)_2$; β -TCP) are currently successfully used in human bone surgery. The aim of this work was to evaluate the influence of the presence of sodium ion in β -TCP on its mechanical and biological properties. Five Na-doped- β -TCP [$\text{Ca}_{10.5-x/2}\text{Na}_x(\text{PO}_4)_7$, $0 \leq x \leq 1$] microporous pellets were prepared via solid phase synthesis, and their physico-chemical data (lattice compacity, density, porosity, compressive strength, infrared spectra) denote an increase of the mechanical properties and a decrease of the solubility when the sodium content is raised. On the other hand, the in vitro study of MC3T3-E1 cell activity (morphology, MTS assay and ALP activity) shows that the incorporation of sodium does not modify the bioactivity of the β -TCP. These results strongly suggest that Na-doped- β -TCP appear to be good candidates for their use as bone substitutes.

1 Introduction

Calcium phosphate materials are biocompatible, capable of bonding chemically to bone [1]. Most of the ceramics used as bone substitute materials are made of calcium phosphate [2, 3] because of their chemical similarity with bone

mineral [4]. Among calcium phosphate ceramics, β -tricalcium phosphate [$\text{Ca}_3(\text{PO}_4)_2$; β -TCP] is currently used with success in human bone surgery. However, such bio-ceramics show limited mechanical properties [5–7], which means a significant amount of research has yet to be done before they can compete with autologous bone grafting procedure, especially in loaded surgical sites.

A possible way to modify both mechanical and biological properties of β -TCP ceramics consists in a partial replacement of calcium by specific elements. For instance, partial Zn for Ca substitutions in the β -TCP lattice can promote bone stimulation [8] and decrease the solubility of the material [9]. Our more recent work was focused on the Na for Ca substitution, previously described in the literature [10]. Chemical routes for synthesizing Na-doped- β -TCP were thus explored and the resulting materials were characterized using both ^{31}P MAS-NMR and XRD methods [11]. In the present work, we report both mechanical and in vitro biological properties of a series of Na-doped- β -TCP [$\text{Ca}_{10.5-x/2}\text{Na}_x(\text{PO}_4)_7$, $0 \leq x \leq 1$], as a function of the Na for Ca substitution rate x . Accordingly, microporous pellets of the considered ceramics were prepared and their structure (atomic compacity, porosity), infrared absorption solubility and hardness were analyzed. The viability and activity (alkaline phosphatase) of an osteoblastic cell line (MC3T3-E1), cultured in contact with various Na-doped- β -TCP pellets, were then studied.

2 Materials and methods

2.1 Synthesis of β -TCP pellets

Syntheses of β -TCP with different Na quantities (Table 1) were performed via solid phase reaction [10]. CaHPO_4 ,

L. Obadia · M. Julien · S. Quillard · T. Rouillon · P. Pilet ·
J. Guicheux · J.-M. Bouler (✉)
INSERM, UMR 791, LIOAD, Faculté de Chirurgie Dentaire,
Université de Nantes, BP 84215, 44042 Nantes Cedex 1, France
e-mail: jean-michel.bouler@univ-nantes.fr

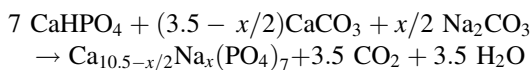
B. Bujoli
CNRS, UMR 6230, CEISAM, UFR Sciences et Techniques,
Université de Nantes, 2 rue de la Houssinière, BP 92208,
44322 Nantes Cedex 3, France

Table 1 Na content in $\text{Ca}_{10.5-x/2}\text{Na}_x(\text{PO}_4)_7$ compounds, determined via AAS

x	Expected Na% (by weight)	Experimental Na% (by weight)
0	0	0.000 ± 0.001
0.25	0.53	0.54 ± 0.01
0.50	1.06	1.07 ± 0.02
0.75	1.59	1.61 ± 0.03
1	2.11	2.13 ± 0.03

CaCO_3 and Na_2CO_3 were crushed in an agate mortar for 30 min.

For each composition, 20 pellets (20 mm of diameter and 5 mm of thickness) were prepared via uniaxial compression. β -TCP microporous ceramics were obtained after sintering the pellets at 1,000°C for 24 h, according to the following reaction:



2.2 β -TCP pellets characterization

The Na content of the β -TCP samples was measured via atomic absorption spectrometry. 100 mg of sample were dissolved in 2 ml of a 10% HCl solution then diluted in a 0.2% KCl solution. Analyses were performed at 589 nm, under an air/acetylene flame with a Na-lamp using an Unicam Solaar 989 atomic absorption spectrometer (Thomas Jarell Ash, Cambridge, UK).

Infrared data were registered with a Nicolet Magna II 550 Fourier transform infra-red spectrometer (4 cm^{-1} resolution and 100 cumulated scans). The samples were pressed in KBr pellets. The spectra were automatically baseline corrected by OMNIC software package (*Omnic 7.1*, Thermo Electron Corporation, Madison, USA).

For each kind of sample, the total porosity and distribution of pores was measured using an Autopore III 940 mercury porosimeter (Micromeritics, USA).

The compressive strength value of the pellets was obtained from Vickers hardness measurements. Both elastic limit (σ_e) and compressive strength (σ_c) are equivalent for ceramics because these materials are brittle without plastic domain. For ceramics, the elastic limit is directly linked to the hardness (H_v) by the following equation: $H_v = 3 \sigma_e = 3 \sigma_c$ [12]. For these reasons, the compressive strength of ceramics can be determined using Vickers indentation. The Vickers indentation measurements were performed on $\text{Ca}_{10.5-x/2}\text{Na}_x(\text{PO}_4)_7$ ($x = 0, 0.25, 0.5, 0.75, 1$) pellets. Each result was an average of ten measurements.

After sintering, the pellets were weighted and their dimensions were measured to obtain their volume. From these data, the apparent density value was determined.

The lattice compacity of $\text{Ca}_{10.5-x/2}\text{Na}_x(\text{PO}_4)_7$ ($0 < x < 1$) was determined from X-ray diffraction (XRD) patterns, recorded using a Philips PW 1830 generator equipped with a vertical PW 1050 ($\theta/2\theta$) goniometer and a PW 1711 Xe detector (Eindhoven, The Netherlands). They were recorded using the copper $K\alpha$ radiation in a step-by-step mode with the following parameters:

2θ initial: 10° , 2θ final: 100° step $2\theta = 0.03^\circ$, time per step: 2.3 s The lattice compacity of each composition was obtained from the following equation:

$$\text{Compacity} = \text{Volume (atoms)} / \text{Volume (lattice cell)}$$

The volume of atoms in the β -TCP lattice was determined from the number of atoms per unit cell and the ionic radius of atoms [13].

The $\text{Ca}_{10.5-x/2}\text{Na}_x(\text{PO}_4)_7$ lattice cell contains $(273 + 3x)$ atoms, and the total atom volume is given by $V_{\text{atom}} = [(V_{\text{Ca}} * (10.5 - x/2)) + (x * V_{\text{Na}}) + ((V_{\text{P}} + (V_{\text{O}} * 4)) * 7)] * 6$. The lattice cell volume was obtained from X-ray diffraction measurements using the Rietveld method. XRD refinements were performed using Winplotr and Fullprof as graphic user interface and as Rietveld refinement software [14, 15]. The precision on the lattice cell parameters were calculated using the formula: $\text{SD} * 3 * \text{Scor}$, where SD is the standard deviation and Scor, a serial correlation coefficient [16].

For the dissolution studies, two 200 mg pellets were immersed in 80 ml of a 0.05 mol l^{-1} acetate buffer (pH 4.8) during 450 min. The calcium concentration was measured using a Ca^{2+} specific electrode (Ion Plus®, model 9320) on 500 μl decanted aliquots collected at regular intervals and the PO_4^{3-} concentration was determined by complexometry. In the latter case, 100 μl of Molybdenum–Vanadium reagent (Merck) were added to 500 μl of the sample, and the absorbance was read at 405 nm with a Secoman S750 UV spectrometer.

2.3 Cell culture

Cell culture plastic ware was purchased from Corning (Corning BV Life Sciences, Schiphol-Rijk, The Netherlands). Fetal calf serum (FCS), α -MEM, L-glutamine, penicillin/streptomycin, trypsin/EDTA and phosphate buffered salt (PBS) were purchased from Invitrogen Corporation (Paisley, UK).

Nonidet P-40 was obtained from Amersham Biosciences (Orsay, France). *P*-nitrophenylphosphate, 2-amino-2-methyl-1-propanol and MgCl_2 were purchased from Sigma (St Louis, MO, USA). 3-(4, 5-Dimethylthiazol-2-yl)-5-(3-carboxymethoxyphenyl)-2-(4-sulphophenyl-2H) tetrazolium inner salt (MTS) was obtained from Promega (Madison, WI, USA).

MC3T3-E1 cells are a non-transformed cell line established from newborn mouse calvaria. These cells exhibit an osteoblastic phenotype as evidenced by the expression of

ALP activity [17], the synthesis of extracellular matrix (ECM) components such as osteocalcin and type-1 collagen [18] and their ability to mineralise the ECM. MC3T3-E1 cells were routinely grown in α -MEM medium supplemented with 10% FCS, 1% penicillin/streptomycin and 1% L-glutamine. Cells were subcultured once a week using trypsin/EDTA and maintained at 37°C in a humidified atmosphere of 5% CO₂ in air. Medium was completely renewed every 2 days.

2.4 Cell morphology

MC3T3-E1 cell morphology was studied in contact with the various material pellets by scanning electron microscopy (SEM). Cells were seeded onto materials in 24-multiwell plates at a final density of 10,000 cells/cm². After indicated times, media were removed and specimens were fixed with 4% glutaraldehyde in PBS (pH 7.2) for 1 h 30 at 4°C. After dehydration in graded alcohols, specimens were treated with graded mixture of ethanol/trichlorotrifluoroethane (75/25, 50/50, 25/75 and 0/100). They were then sputter-coated with gold–palladium. The surface of specimen was finally examined with secondary electrons in SEM under 15 kV voltage [19].

2.5 Cell viability

Cell viability was measured as mitochondrial NADH/NADPH-dependent dehydrogenase activity, resulting in the cellular conversion of the tetrazolium salt MTS into a soluble formazan dye [20, 21] with the CellTiter 96 aqueous non-radioactive cell proliferation assay (Promega). MC3T3-E1 cells were cultured on the surface of β -TCP or Na-doped β -TCP pellets (direct contact). In addition, MC3T3-E1 cells were cultured on plastic in the presence of the two materials, using transwell inserts. Transwell inserts are culture chambers in which materials were placed before being immersed in 24-multiwell plates. MC3T3-E1 cells cultured on plastic in the absence of materials were used as control. Cells were seeded at a density of 10,000 cells/cm². After indicated times, culture media were removed and 100 μ l of MTS solution was added in each well for 2–3 h according to the manufacturer's instructions. Finally, colorimetric measurement of formazan dye was performed on a spectrophotometer with an OD reading at 490 nm. Results were expressed as a relative MTS activity as compared to the control conditions (cells cultured in the absence of materials).

2.6 Alkaline phosphatase (ALP) activity

ALP activity was evaluated, as previously described [22], in MC3T3-E1 cells (24-multiwell plates, 10,000 cells/cm²) cultured either onto the β -TCP or Na-doped β -TCP pellets or

without direct contact using transwell inserts as described above. Cells cultured on plastic in the absence of material were used as control. After indicated times, cells were washed twice with ice-cold PBS and scraped in 0.2% aqueous solution of Nonidet P-40. Cell suspension was then sonicated on ice for 30 s and centrifuged for 5 min at 4°C. Aliquots of supernatants were subjected to protein assay with the Pierce coomassie plus assay reagent (Pierce, Rockford, USA) and to ALP activity measurement. ALP activity was assessed at pH 10.3 in 0.1 M 2-amino-2methyl-1-propanol containing 1 mM MgCl₂. P-NPP (10 mM) was used as a chromogenic substrate for an optical density reading at 405 nm. Results were expressed as relative ALP activity compared with control conditions (cells cultured in the absence of material).

2.7 Statistical analysis

Each experiment was performed thrice with similar results. Results are expressed as mean \pm SEM of triplicate determinations. Comparative studies of means were performed using one-way ANOVA followed by a post hoc test (Fisher projected least significant difference) with a statistical significance at $P < 0.05$.

3 Results

3.1 Na-doped β -TCP pellets characterization

From atomic absorption analyses the Na content of the Ca_{10.5-x/2}Na_x(PO₄)₇ [$0 \leq x \leq 1$] phases was found to be close to the expected values (Table 1). A non-parametric Kolmogorov–Smirnov test has been performed and according to the variability of measurements (see experimental errors in Table 1) no significant differences ($P > 0.9$) were put in evidence between expected and experimental distributions.

Mercury porosity studies showed that the total porosity of pure β -TCP pellets is higher, compared with Ca₁₀Na(PO₄)₇. Distribution of pores, determined using a mercury porosimeter, revealed that more than 98% of pores have a diameter smaller than 10 μ m. However, the pore size distribution differed according to the Na content in the β -TCP phases: Na-doped β -TCPs contains a higher amount of small pores (with diameters less than 1 μ m) when compared with pure β -TCP (Fig. 1).

Vickers indentation measurements were performed on pellets for the series of β -TCP containing sodium, Ca_{10.5-x/2}Na_x(PO₄)₇ ($x = 0, 0.25, 0.5, 0.75, 1$). A linear increase of the compressive strength ($P < 0.006$) was clearly observed as the Na content was raised (Fig. 2). For the higher Na-substitution (32.2 MPa, $x = 1$), the correlated compressive strength was

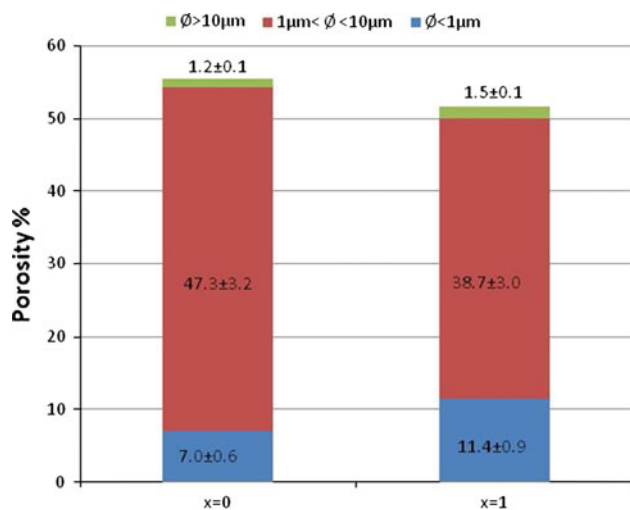


Fig. 1 Total porosity and pore size distribution of $\text{Ca}_{10.5-x/2} \text{Na}_x(\text{PO}_4)_7$ (Na-doped β -TCP $x = 1$; pure β -TCP $x = 0$), determined using a mercury porosimeter. Each proportions are averaged over five samples

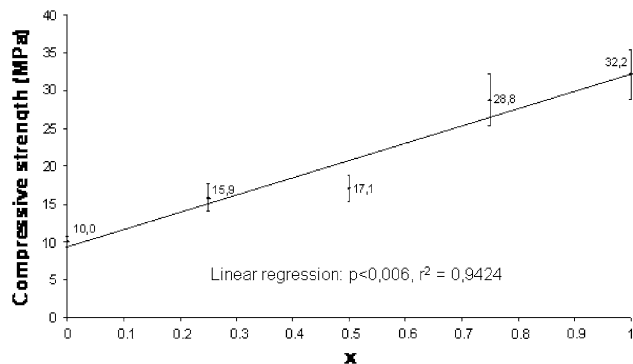


Fig. 2 Compressive strength of $\text{Ca}_{10.5-x/2} \text{Na}_x(\text{PO}_4)_7$ ($x = 0, 0.25, 0.5, 0.75, 1$) as a function of the x sodium content. Each data was the average of ten measurements

three times as high as that measured for pure β -TCP (10 MPa, $x = 0$). Indeed, increasing the Na content resulted in a higher density of the β -TCP sintered pellets (from 1.6 ($x = 0$) to 1.7 ($x = 1$))—Fig. 3) and a decrease of the optimal sintering temperature value. This is likely related to the observed linear increase ($P < 0.00001$) in the atomic compacity (from 0.623 ($x = 0$) to 0.628 ($x = 1$))—Fig. 4), concomitant with a decrease of the unit cell volume and an increase of the atom volume in the unit cell, when x varies from 0 to 1.

In addition, $\text{Ca}_{10.5-x/2} \text{Na}_x(\text{PO}_4)_7$ ($x = 0, 0.5, 1$) pellets were soaked in a pH 4.8 acetate buffer, to compare their relative dissolution speed versus time over a 450 min period. The dissolution of Na-doped β -TCPs was found to be slower than pure β -TCP, as evidenced by the release profiles of calcium (Fig. 5) and phosphate ions (data not shown).

In Fig. 6 the infrared spectra of pure β -TCP ($x = 0$) and Na-doped β -TCP ($x = 1$) are presented in the $1400\text{--}450 \text{ cm}^{-1}$

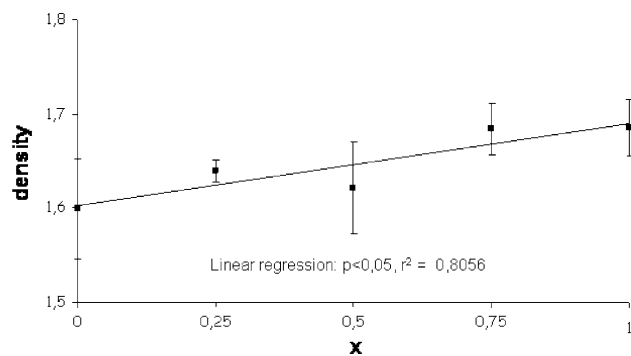


Fig. 3 Apparent density of $\text{Ca}_{10.5-x/2} \text{Na}_x(\text{PO}_4)_7$ pellets after sintering

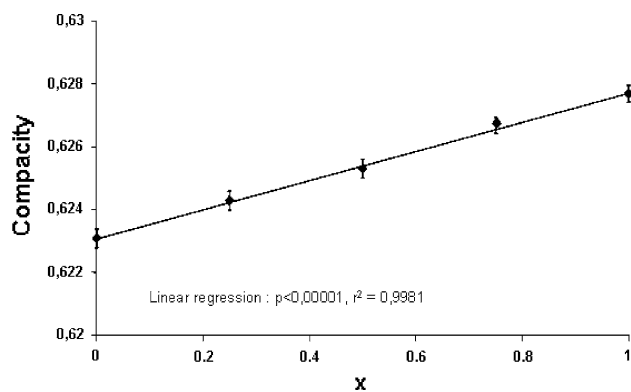


Fig. 4 Compacity of $\text{Ca}_{10.5-x/2} \text{Na}_x(\text{PO}_4)_7$ ($x = 0, 0.25, 0.5, 0.75, 1$)

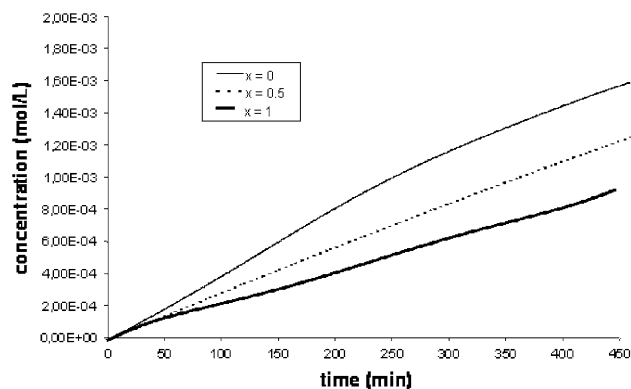


Fig. 5 Ca^{2+} ions release profile for $\text{Ca}_{10.5-x/2} \text{Na}_x(\text{PO}_4)_7$ ($x = 0, 0.5, 1$) pellets soaked in a pH 4.8 acetate buffer

frequency range. The complete series of spectra is presented elsewhere [23]. Two groups of bands are clearly seen corresponding to some of the normal modes of the phosphates groups PO_4^{3-} : $\nu_1\text{--}\nu_3$ stretching modes ($1200\text{--}900 \text{ cm}^{-1}$) and ν_4 bending modes ($500\text{--}650 \text{ cm}^{-1}$). Main observed bands are picked on the spectra of fully doped sample. The values are found close to those previously reported for β -TCP [24, 25].

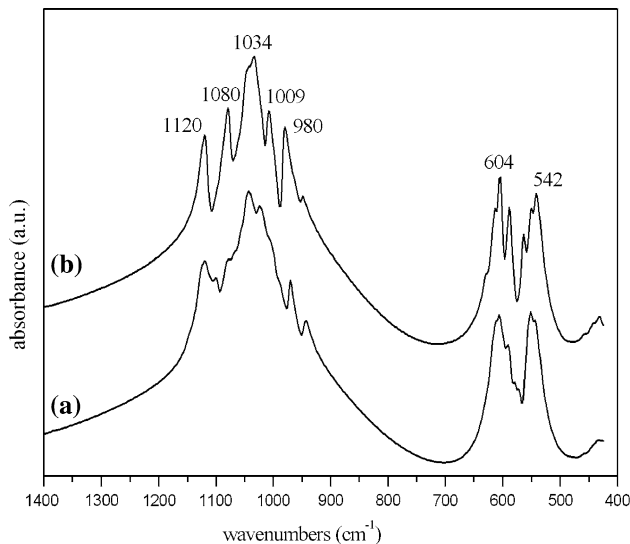


Fig. 6 Infrared spectra of $\text{Ca}_{10.5-x/2} \text{Na}_x(\text{PO}_4)_7$ for **a** pure β -TCP ($x = 0$) and **b** Na-doped β -TCP ($x = 1$)

3.2 Cell morphology

Scanning electron microscopic images of osteoblastic MC3T3-E1 cells cultured for 48 h on $\text{Ca}_{10.5-x/2} \text{Na}_x(\text{PO}_4)_7$ ($x = 0, 1$) materials, showed that cells were adhering onto both phases, with a flattened and elongated morphology (Fig. 7). For the two materials, cells were spread on the whole surface and presented numerous cytoplasmic extensions and lamellopodia. These results indicate that the cell morphology was not significantly affected by the presence of sodium in β -TCP.

3.3 Cell viability

To analyze the viability of osteoblasts, the MTS activity of MC3T3-E1 cells was measured, when cultured either directly onto $\text{Ca}_{10.5-x/2} \text{Na}_x(\text{PO}_4)_7$ ($x = 0, 1$) pellets or on plastic in the presence (via transwell inserts) or absence of the materials (control conditions). The MTS activity was

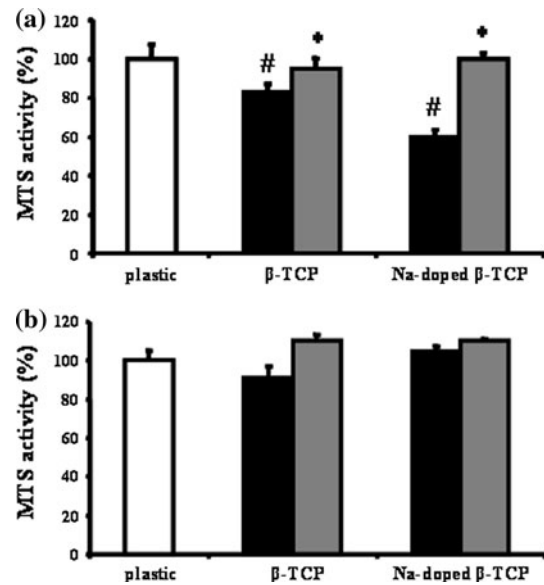


Fig. 8 MTS activity of MC3T3-E1 cells cultured directly onto $\text{Ca}_{10.5-x/2} \text{Na}_x(\text{PO}_4)_7$ (Na-doped β -TCP $x = 1$; pure β -TCP $x = 0$) pellets (black) or using transwell inserts (grey) for 7 days (a) and 14 days (b) (see Materials and methods). Results are expressed in relative MTS activity compared with control conditions (plastic). * $P < 0.05$ ($n = 3$) as compared to β -TCP or Na-doped β -TCP under direct contact conditions, # $P < 0.01$ ($n = 3$) as compared to control conditions (plastic)

evaluated after one- and two-weeks of culture. Results indicated that after 1 week, the MTS activity was significantly reduced by about 30 and 38% ($P < 0.05$) when the cells were directly cultured on $\text{Ca}_{10.5} \text{Na}(\text{PO}_4)_7$ and $\text{Ca}_{10.5-x/2} \text{Na}_x(\text{PO}_4)_7$ pellets respectively, as compared to control conditions (Fig. 8a). In contrast, the cell viability observed without direct contact, using transwell inserts, was not statistically different from that recorded under control conditions.

After 2 weeks, no significant difference in the cellular viability of osteoblasts was noted whatever the culture conditions (Fig. 8b). These results show that the osteoblast

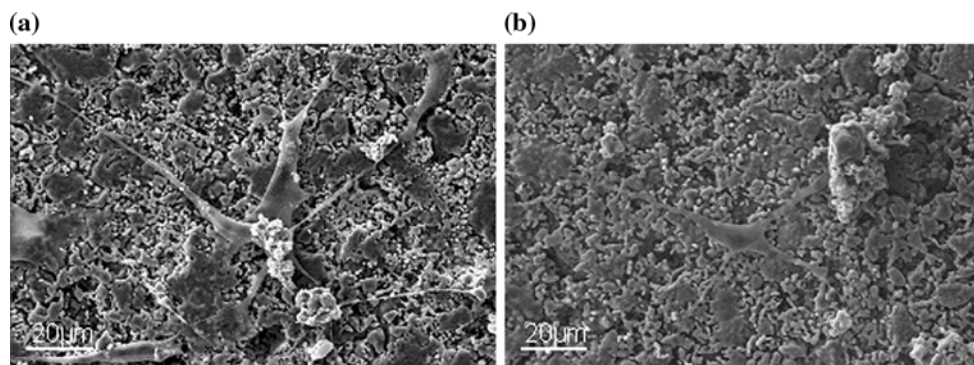


Fig. 7 SEM images of MC3T3-E1 cells, cultured for 48 h onto $\text{Ca}_{10.5-x/2} \text{Na}_x(\text{PO}_4)_7$ $x = 0$ (a), 1 (b) pellets. Samples were observed using secondary electrons (magnification = 750)

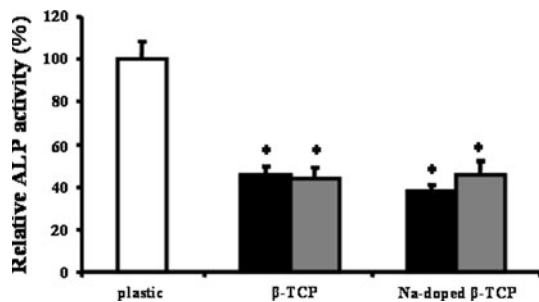


Fig. 9 ALP activity of MC3T3-E1 cells cultured directly onto $\text{Ca}_{10.5-x/2}\text{Na}_x(\text{PO}_4)_7$ (Na-doped β -TCP $x = 1$; pure β -TCP $x = 0$) pellets (black) or using transwell inserts (grey) for 14 days (see Materials and methods). Results are expressed in relative ALP activity compared with control conditions (plastic). * $P < 0.0001$ ($n = 3$) as compared to control conditions (plastic)

viability decreased after 1 week when cultured in direct contact with the $\text{Ca}_{10.5-x/2}\text{Na}_x(\text{PO}_4)_7$ ($x = 0, 1$) pellets, while this reduction was almost completely recovered after 2 weeks.

3.4 ALP activity

The potential influence of the $\text{Ca}_{10.5-x/2}\text{Na}_x(\text{PO}_4)_7$ ($x = 0, 1$) materials on the osteoblastic ALP activity was then examined, using osteoblasts cultured for 2 weeks either directly onto the materials or on plastic in the presence (via transwell inserts) or absence of the materials (control conditions). Figure 9 shows that culturing cells in the presence of the materials (in direct or indirect contact via transwell inserts) induced a twofold decrease in ALP activity as compared to plastic conditions. Interestingly, the Na-doped β -TCP failed to induce a significant change in ALP activity as compared to β -TCP. These results indicate that osteoblasts maintained their capacity to express ALP whatever the culture conditions.

4 Discussion

Incorporation of heteroatoms in calcium phosphates can influence their mechanical properties, solubility and bio-activity [26, 27], that are critical features for their use as bone substitutes. In previous studies we have demonstrated that sodium ions can be incorporated in the β -TCP lattice using solid phase syntheses from CaHPO_4 , CaCO_3 and Na_2CO_3 [11]. This procedure allows a fine tuning of the Na content in β -TCP, and recent experiments confirmed that the sodium ions are homogeneously incorporated in the lattice [11]. Moreover, the selected sintering process was adapted to avoid the presence of cracks in the resulting microporous $\text{Ca}_{10.5-x/2}\text{Na}_x(\text{PO}_4)_7$ ($x = 0, 0.25, 0.5, 0.75, 1$) pellets. Our purpose was to evaluate the influence of the

sodium incorporation in β -TCP microporous pellets, on their physical, chemical and biological properties.

In previous studies, we have shown that Vickers indentation is a non destructive method that can be used to determine the compressive strength for this kind of materials [28, 29] and to probe the homogeneity of samples, by performing measurements at several points of the surface. In the present case, a linear increase of the compressive strength was clearly observed as the Na content was raised. Better mechanical properties of synthetic bone substitute can induce at least a better handle of macroporous ceramics by surgeons. This result is consistent with the concomitant (i) increase of the pellets density (ii) decrease of total porosity (Na-doped β -TCP contain smaller pores compared to pure β -TCP) (iii) increase of the lattice compacity. The slower dissolution of the Na-doped β -TCP samples in acidic buffer, is probably due to a less important contact surface available or to the different chemical composition of the compounds.

Dilatometry experiments are in progress to describe the kinetics of the pellets densification as a function of temperature. The increase of the sodium amount in the samples likely facilitates the sintering process, as a result of a higher ionic mobility.

The frequencies of infrared bands are very similar in the pure β -TCP and in the fully Na-doped sample confirming that no strong changes occur in the crystal structure upon doping. For the fully doped compound, the bands at 1120, 1080, 1034 and 1009 cm^{-1} can be attributed to the anti-symmetric stretching (ν_3) mode, and the band at 980 cm^{-1} to symmetric stretching vibration (ν_1) of the tetrahedra. The ν_4 antisymmetric bending vibrations give the frequencies around 604 and 542 cm^{-1} . However, in the case of Na-doped TCP, one can observe that the bands are less numerous and more resolved than for pure compound. This observation could indicate a lower local disorder leading to a better compacity of the structure. Keeping in mind that the vibration modes are sensitive to the local environment of the phosphate groups, this is consistent with the effect of Na-substitution. In the pure β -TCP, it has been shown that five different phosphate groups are present and that vacancies are present on one of the calcium sites. The Na-substitution lead to complete filling of the vacancies and, consequently, only three distinct phosphates are evidenced in Na-doped TCP [11].

Apatite-containing bioactive implants are slowly replaced by natural bone tissue formed by osteoblasts, which are key regulatory cells that regulate bone cell differentiation. Among the cellular models mimicking the various stages of osteoblastic differentiation in a temporally regulated manner, the clonal osteogenic cell line MC3T3-E1 is one of the most widely used since it is a non-transformed cell line that expresses a high alkaline phosphatase

activity in the confluent state and mineralizes the extracellular matrix *in vitro* [18]. Interestingly, as a non-transformed cell line, MC3T3-E1 fail to exhibit low sensitivity to cytotoxic signals as obviously observed with transformed cell lines.

In this context, we first examined by SEM the morphology of MC3T3-E1 cells cultured on the surface of $\text{Ca}_{10.5-x/2}\text{Na}_x(\text{PO}_4)_7$ ($x = 0, 1$) pellets for 2 days. The cells formed flattened sheets on the smooth regions of the pellets and exhibited large cytoplasmic extensions suggesting an active cell migration. For both materials, the chemical nature of the surface may provide sites for focal adhesion molecules of the cells such as integrins [30]. It might be useful to further analyze the cell adhesion process to get further insights in the role of the chemical nature of the surface of the $\text{Ca}_{10.5-x/2}\text{Na}_x(\text{PO}_4)_7$ materials, in these cellular phenomena.

To investigate the effect of the presence of sodium in β -TCP on the viability of osteoblasts, the mitochondrial dehydrogenase activity (MTS activity) of MC3T3-E1 cells was measured, according to standards (ISO 10993-5: Biological evaluation of medical devices-Part 5: Tests for *in vitro* cytotoxicity), when cultured in contact (direct or indirect via transwell inserts) with pellets of pure β -TCP and $\text{Ca}_{10}\text{Na}(\text{PO}_4)_7$ bioceramics. The decrease in cell viability observed at early stage of culture (day 7) was almost not present under longer-term culture conditions (14 days). This data strongly suggest that the Na-doping of β -TCP did not dramatically influence the cells viability. The observed transient alteration of cell viability could be related to a cellular sensitivity to the surface topography or composition [31], since indirect contact culture conditions, via transwell inserts, did not lead to a similar behavior.

In addition, when exposed to an aqueous biological medium, dissolution of surface ions can take place, followed by the formation of a hydroxyapatite (HA) layer on the surface of the pellets [32]. Since it was reported that this feature might induce some cytotoxic effects [33], it would be interesting to investigate whether β -TCP and Na-doped β -TCP pellets release some cytotoxic derivatives, at least in the early stages of the culture. Furthermore, some reports have identified proteins involved in the adhesion of osteoblasts on biomaterials [30]. Adsorption of proteins from the serum and other constituents present in the culture wells might modify the chemical composition at the solid–liquid interface and accordingly might influence the cellular adhesion and proliferation [34].

The ALP activity is one of the most widely used osteoblastic markers [35], and we have tested whether MC3T3-E1 cells preserve their phenotype when contacted with β -TCP and Na-doped β -TCP. As previously mentioned for cell viability, the decreased ALP activity might be related to the release of ionic elements [33], such as phosphate and calcium ions, when the biomaterials are

soaked in the culture medium, that might affect *in vitro* osteoblast survival. Indeed, it has been shown that phosphate ions cause a dose- and time-dependent increase in apoptosis of epiphyseal [36] chondrocytes [20] and osteoblasts [37, 38], which may contribute to terminal differentiation of these cells. High phosphate and calcium concentrations are known to influence the ALP activity [39]. Work is currently in progress to determine the phosphate and calcium concentrations released from the materials under culture conditions. There is still a great deal left to understand and learn about the role of ions in cellular metabolic activity, for the rational design of biomaterials for which the local phosphate and calcium concentrations released could be controlled, at levels that ensure cellular viability and promote differentiation.

5 Conclusion

This work demonstrate that the incorporation of sodium ions within the β -TCP lattice significantly increases the compressive strength of microporous pellets of this bioceramic without modifying its *in vitro* bioactivity. These results strongly suggest that Na-doped- β -TCP appear to be good candidates for their use as bone substitutes. However, macroporous ceramics are needed to favour the penetration of cells and biological fluids for *in vivo* implantations. Accordingly, we are currently investigating the comparative behaviour of macroporous pure β -TCP and Na-doped β -TCP ceramics, using *in vivo* implantations in rabbits.

Acknowledgment This work was supported by CNRS “Programme Matériaux Nouveaux, Nouvelles Fonctionnalités”, Région Pays de Loire “Programme Biomatériaux S3” and Fondation Avenir pour la Recherche Médicale appliquée, étude ET2-321. Marion Julien received a fellowship from INSERM and region des Pays de la Loire.

References

1. LeGeros JP. Biodegradation and bioresorption of calcium phosphate ceramics. *Clin Mater.* 1993;14:65–88.
2. Cavagna R, Daculsi G, Bouler J. Macroporous calcium phosphate ceramic: a prospective study of 106 cases in lumbar spinal fusion. *J Long Term Eff Med Implants.* 1999;9:403–12.
3. Ransford A, Morley T, Edgar M, Webb P, Passuti N, Chopin D, et al. Synthetic porous ceramic compared with autograft in scoliosis surgery. A prospective, randomized study of 341 patients. *J Bone Joint Surg Br.* 1998;80:13–8.
4. Rey C. Calcium phosphate biomaterials and bone mineral. Differences in composition, structures and properties. *Biomaterials.* 1990;11:13–5.
5. Bouler J-M, Trécant M, Delécrin J, Royer J, Passuti N, Daculsi G. Macroporous biphasic calcium phosphate ceramics: influence of five synthesis parameters on compressive strength. *J Biomed Mater Res.* 1996;32:603–9.

6. Pecqueux F, Tancret F, Payraudeau N, Bouler J-M. Influence of microporosity and macroporosity on the mechanical properties of biphasic calcium phosphate bioceramics: modelling and experiment. *J Eur Ceram Soc.* 2010;30:819–29.
7. Perera FH, Martinez-Vazquez FJ, Miranda P, Ortiz AL, Pajares A. Clarifying the effect of sintering conditions on the microstructure and mechanical properties of beta-tricalcium phosphate. *Ceram Int.* 2010;36(6):1929–35.
8. Kawamura H, Ito A, Miyakawa S, Layrolle P, Ojima K, Ichinose N, et al. Stimulatory effect of zinc-releasing calcium phosphate implant on bone formation in rabbit femora. *J Biomed Mater Res.* 2000;50(2):184–90.
9. Ito A, Kawamura H, Miyakawa S, Layrolle P, Kanzaki N, Treboux G, et al. Resorbability and solubility of zinc-containing tricalcium phosphate. *J Biomed Mater Res.* 2002;60:224–31.
10. Lazoryak BI, Strunenkov TV, Golubev VN, Vovk EA, Ivanov LN. Triple phosphates of calcium, sodium and trivalent elements with whitlockite-like structure. *Mater Res Bull.* 1996;31(2):207–16.
11. Obadia L, Deniard D, Alonso B, Rouillon T, Jobic S, Guicheux J, et al. Effect of sodium doping in β -tricalcium phosphate on its structure and properties. *Chem Mater.* 2006;18:1425–33.
12. Tabor D. The hardness of solids. *Rev Phys Technol.* 1970;1:145–79.
13. Shannon R. Revised effective ionic radii and systematic studies of interatomic distances in halides and chalcogenides. *Acta Cryst A.* 1976;32(5):751–67.
14. Rodriguez-Carvajal J, Roisnel T. Fullprof.98 and WinPLOTR: New Windows 95/NT application for diffraction. Commission for powder diffraction, international union of crystallography 1998; newsletter n 20.
15. Rodriguez-Lorenzo LM, Hart JN, Gross KA. Influence of fluorine in the synthesis of apatites. Synthesis of solid solutions of hydroxy-fluorapatite. *Biomaterials.* 2003;24(21):3777–85.
16. Berar JF, Lelann P. E.S.D's and estimated probable error obtained in Rietveld refinement with local correlation. *J Appl Cryst.* 1991;24:1–5.
17. Guicheux J, Lemonnier J, Ghayor C, Suzuki A, Palmer G, Caverzasio J. Activation of p38 mitogen-activated protein kinase and c-Jun-NH2-terminal kinase by BMP-2 and their implication in the stimulation of osteoblastic cell differentiation. *J Bone Miner Res.* 2003;18(11):2060–8.
18. Suzuki A, Ghayor C, Guicheux J, Magne D, Quillard S, Kakita A, et al. Enhanced expression of the inorganic phosphate transporter Pit-1 is involved in BMP-2-induced matrix mineralization in osteoblast-like cells. *J Bone Miner Res.* 2006;21(5):674–83.
19. Citeau A, Guicheux J, Vinatier C, Layrolle P, Nguyen TP, Pilet P, et al. In vitro biological effects of titanium rough surface obtained by calcium phosphate grid blasting. *Biomaterials.* 2005;26(2):157–65.
20. Julien M, Khairoun I, LeGeros RZ, Delplace S, Pilet P, Weiss P, et al. Physico-chemical-mechanical and in vitro biological properties of calcium phosphate cements with doped amorphous calcium phosphates. *Biomaterials.* 2007;28:956–65.
21. Relic B, Guicheux J, Mezin F, Lubberts E, Togninalli D, Garcia I, et al. IL-4 and IL-13, but not IL-10, protect human synovocytes from apoptosis. *J Immunol.* 2001;166(4):2775–82.
22. Verron E, Masson M, Khoshniat S, Duplomb L, Wittrant Y, Baud'huin M, et al. Gallium modulates osteoclastic bone resorption in vitro without affecting osteoblasts. *Br J Pharmacol.* 2010;159:1681–92.
23. Quillard S, Obadia L, Deniard P, Bujoli B, Bouler JM. Vibrational properties of sodium substituted β -tricalcium phosphate. *Key Eng Mater.* 2008;361–363:75–8.
24. Rey C, Shimizu M, Collins B, Glimcher MJ. Resolution-enhanced Fourier transform infrared spectroscopy study of the environment of phosphate ions in the early deposits of a solid phase of calcium-phosphate in bone and enamel, and their evolution with age. I: Investigations in the ν_4 PO₄ domain. *Calcif Tissue Int.* 1990;46:384–94.
25. Rey C, Shimizu M, Collins B, Glimcher MJ. Resolution-enhanced Fourier transform infrared spectroscopy study of the environment of phosphate ions in the early deposits of a solid phase of calcium-phosphate in bone and enamel, and their evolution with age. I: Investigations in the ν_3 PO₄ domain. *Calcif Tissue Int.* 1991;49:383–8.
26. Elliott JC. Structure and chemistry of the apatites and other calcium phosphates. *Studies in inorganic chemistry.* Amsterdam: Elsevier; 1994. p. 389.
27. LeGeros RZ. Calcium phosphate in oral biology and medicine. In: Myers HM, editor. *Monograph in oral science.* Switzerland: Karger; 1991. p. 1–201.
28. Collin I, Lamy B, Gauthier O, Bouler J-M. Improvement of macroporous biphasic phosphocalcic ceramics for the filling of bone defects. *ITBM-RBM.* 2005;26(4):247–8.
29. Gauthier O, Muller R, von Stechow D, Lamy B, Weiss P, Bouler J-M, et al. In vivo bone regeneration with injectable calcium phosphate biomaterial: a three-dimensional micro-computed tomographic, biomechanical and SEM study. *Biomaterials.* 2005;26(27):5444–53.
30. Anselme K. Osteoblast adhesion on biomaterials. *Biomaterials.* 2000;21(7):667–81.
31. Boyan BD, Schwartz Z, Lohmann CH, Sylvia VL, Cochran DL, Dean DD, et al. Pretreatment of bone with osteoclasts affects phenotypic expression of osteoblast-like cells. *J Orthop Res.* 2003;21(4):638–47.
32. Bouler J-M, Daculsi G. In vitro carbonated apatite precipitation on biphasic calcium phosphate pellets presenting various HA-/TCP ratios. *Key Eng Mater.* 2001;192–195:119–22.
33. Kokubo T, Kim HM, Kawashita M, Nakamura T. Process of calcification on artificial materials. *Z Kardiol.* 2001;90(3):86–91.
34. Xavier SP, Carvalho PS, Beloti MM, Rosa AL. Response of rat bone marrow cells to commercially pure titanium submitted to different surface treatments. *J Dent.* 2003;31(3):173–80.
35. Chesmel KD, Clark CC, Brighton CT, Black J. Cellular responses to chemical and morphologic aspects of biomaterial surfaces. II. The biosynthetic and migratory response of bone cell populations. *J Biomed Mater Res.* 1995;29(9):1101–10.
36. Deligianni DD, Katsala ND, Koutsoukos PG, Missirlis YF. Effect of surface roughness of hydroxyapatite on human bone marrow cell adhesion, proliferation, differentiation and detachment strength. *Biomaterials.* 2001;22(1):87–96.
37. Maeno S, Niki Y, Matsumoto H, Morioka H, Yatabe T, Funayama A, et al. The effect of calcium ion concentration on osteoblast viability, proliferation and differentiation in monolayer and 3D culture. *Biomaterials.* 2005;26(23):4847–55.
38. Meleti Z, Shapiro IM, Adams CS. Inorganic phosphate induces apoptosis of osteoblast-like cells in culture. *Bone.* 2000;27(3):359–66.
39. Farley JR, Hall SL, Tanner MA, Wergedal JE. Specific activity of skeletal alkaline phosphatase in human osteoblast-line cells regulated by phosphate, phosphate esters, and phosphate analogs and release of alkaline phosphatase activity inversely regulated by calcium. *J Bone Miner Res.* 1994;9(4):497–508.